

Supplements

Realignment

The next processing step arises in response to potential misalignment of the channels along the fiber. For the majority of our dataset, the spatial sampling is 0.255 meters. This leads to an ambiguity in exactly where the strain is being sensed, which could be ± 0.255 m from the measurement point. We adopt the approach of Madjdabadi et al. (2016) who address this issue through a process of ‘realignment’. The measurement $\Delta\nu_i = \nu_{i,j} - \nu_{i,1}$ at channel i and time j is compared to the two adjacent possible changes in absolute Brillouin frequency shift: $\Delta\nu_{i-1} = \nu_{i-1,j} - \nu_{i,1}$ and $\Delta\nu_{i+1} = \nu_{i+1,j} - \nu_{i,1}$. The lowest of these three values is accepted as the final, realigned measurement $\Delta\nu_i$. By applying this algorithm to each time sample, the affect of their observed misalignments was ameliorated.

Gain shifts

Finally, we cleaned a number of artifacts in the dataset resulting from bulk shifts in the intensity of the backscattered light (i.e. gain; Figure S1). These bulk shifts in gain often correlate with bulk shifts in the absolute frequency measured at the interrogator box. In theory, these two values should not be related, but we suspect that there may be a relation between the bulk shifts and the fitting of the Brillouin gain spectrum for each measurement point. Estimation of the peak Brillouin gain, and therefore the Brillouin frequency shift on which the strain measurement relies, is done via a parabolic fitting of the gain spectrum. If the gain is low, and the shape of the spectrum relatively flat and broad, the fitting procedure may be less precise, resulting in the apparent frequency shifts seen in Figure S1, where no real change in strain has occurred. The cause of these shifts is difficult to assess, but they likely happen when portions of the cables that lie in cable trays along the gallery walls are jostled. In particular, we suspect that connectors (not splices) between different cables, when disturbed, can influence the intensity of light returning to the interrogator box, thus producing changes in gain.

To address this, we apply a simple algorithm wherein we identify the bulk gain shifts as any measurement point where the gain changed by 0.014% or greater relative to the previous measurement. At each of these points, we then remove the corresponding strain change from all of the subsequent measurements at that channel.

| Period | Spatial resolution [m] | Spatial sampling [m] | Temporal sampling [min] | Averaging | Frequency start [GHz] | Frequency stop [GHz] | Frequency step [MHz] |
|--------------------|------------------------|----------------------|-------------------------|-----------|-----------------------|----------------------|----------------------|
| Gallery excavation | 1.0 | 0.26 | 60 | 3000 | 10.5 | 11.1 | 0.5 |

Table 1. DITEST configuration parameters during the various phases of measurement detailed below. Note that that spatial resolution was changed during the pulse-step test due to high noise levels.

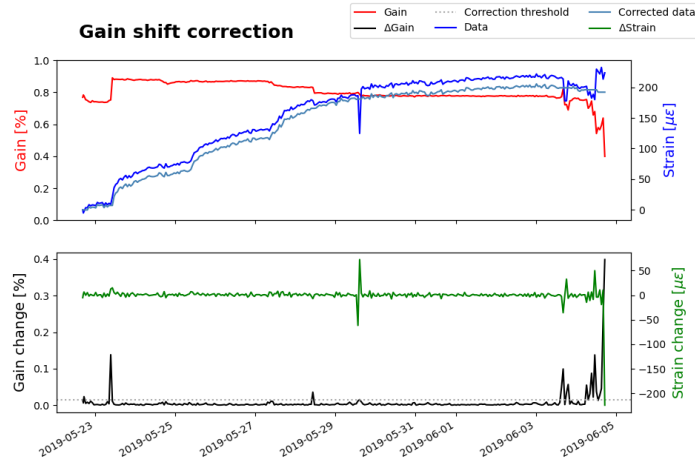


Figure 1. Example channel from BCS-D5 showing A) Gain in red and relative strain in blue prior to the correction for bulk shifts. Light blue shows the corrected data with no shifts at the time of bulk jumps in the gain. B) Shows the differentials of the relative strain in green and gain in black. When gain change exceeded the dotted line (0.014%), we subtracted the change in strain (green) from all subsequent strain measurements (blue).

32

Core evidence for DSS anomalies

33

Figure 2 shows core scanner images from the three off-fault intervals in BCS-D3 and D5 that displayed DSS anomalies. The exact intervals are indicated in red boxes.

34

35

References

36

Madjdabadi, B., Valley, B., Dusseault, M. B., & Kaiser, P. K. (2016, jan). Experimental evaluation of a distributed Brillouin sensing system for measuring extensional and shear deformation in rock. *Measurement*, *77*, 54–66. Retrieved from <https://doi.org/10.1016/j.measurement.2015.08.040> doi: 10.1016/j.measurement.2015.08.040

37

38

39

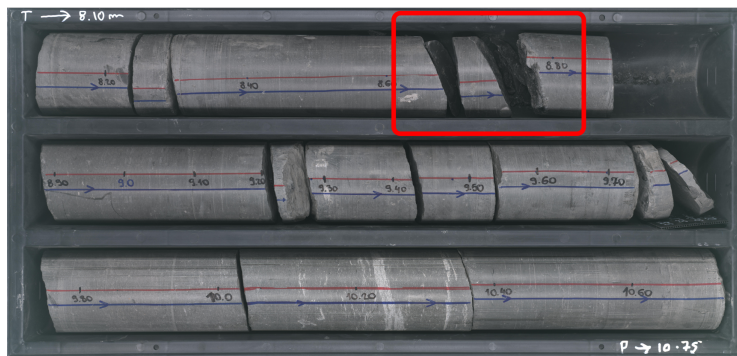
40

41

BCS-D3: 14-17 m



BCS-D5: 8-11 m



BCS-D5: 13-16 m



Figure 2. Core scans of the off-fault intervals that displayed measurable strains on the DSS.

No core was taken from BCS-D4 and no off-fault anomalies were observed in BCS-D6.